IEEE Access
Multidisciplinary | Rapid Review | Open Access Journal

Received July 13, 2020, accepted July 20, 2020, date of publication August 3, 2020, date of current version August 14, 2020.

*Digital Object Identifier 10.1109/ACCESS.2020.3013596*

# Optimal Design of a Hybrid Energy Storage System in a Plug-In Hybrid Electric Vehicle for Battery Lifetime Improvement

**YUNFEI BAI[1,2], (Student Member, IEEE), JIANWEI LI[1,2], (Member, IEEE), HONGWEN HE[1,2], (Senior Member, IEEE), RICARDO CANELOI DOS SANTOS[3], (Member, IEEE), AND QINGQING YANG[4], (Member, IEEE)**

[1]National Engineering Laboratory for Electric Vehicles, School of Mechanical Engineering, Beijing Institute of Technology (BIT), Beijing 100081, China
[2]Collaborative Innovation Center of Electric Vehicles in Beijing, School of Mechanical Engineering, Beijing Institute of Technology (BIT), Beijing 100081, China
[3]Center for Engineering, Modeling and Social Science, Federal University of the ABC, Santo André 09210-580, Brazil
[4]Faculty of Engineering, Environment and Computing, Coventry University, Coventry CV1 5FB, U.K.

Corresponding author: Jianwei Li (jianwei.li@bath.edu)

This work was supported by the Nature Science Foundation of China under Grant 51807008 and Grant U1864202.

**ABSTRACT** This paper proposes a multi-dimensional size optimization framework and a hierarchical energy management strategy (HEMS) to optimize the component size and the power of a plug-in hybrid electric vehicle (PHEV) with the hybrid energy storage system (HESS). In order to evaluate the performance of size optimization and power optimization, a PHEV with a battery energy storage system (BESS) is used as a comparison reference, and the dynamic programming (DP) algorithm is set as a benchmark for comparison. The size optimization method explores the optimal configuration of the system, including the maximum power of the system, the maximum power and capacity of the battery, and the maximum power and capacity of the supercapacitor (SC). Compared with the BESS, the size-optimized HESS reduces the capacity of the system by 31.3% and improves the economy by 37.8%. The HEMS can simultaneously optimize vehicle fuel consumption and suppress battery aging. Its upper layer uses the DP algorithm to optimize fuel economy, and the lower layer apply the linear programming (LP) method to improve battery life. Based on the size optimization results and HEMS, compared with the benchmark, the battery aging rate has been reduced by 48.9%, and the vehicle economy has increased by 21.2%.

**INDEX TERMS** Battery life improvement, hybrid energy storage system, plug-in hybrid electric vehicle, power optimization, size optimization.

## NOMENCLATURE

| | |
|---|---|
| PHEV | Plug-in hybrid electric vehicle |
| SC | Supercapacitor |
| HESS | Hybrid energy storage system |
| BESS | Battery energy storage system |
| EMS | Energy management strategy |
| ESU | Energy storage unit |
| DP | Dynamic programming |
| HEMS | Hierarchical energy management strategy |
| LP | Linear programming |
| ICE | Internal combustion engine |
| ISG | Integrated starter generator |
| TM | Traction motor |
| B-PHEV | PHEV with BESS |
| H-PHEV | PHEV with HESS |
| ODP | Optimal DP |
| NDP | Naïve DP |
| CTUDC | Chinese typical urban driving cycle |

The associate editor coordinating the review of this manuscript and approving it for publication was F. R. Islam.

## I. INTRODUCTION

With the increasing awareness of global warming, energy shortages and environmental pollution have aroused people's attention in the field of vehicles [1]. Exhaust emissions from traditional internal combustion engine vehicles are one of the main factors contributing to this crisis [2], [3]. The plug-in hybrid electric vehicle (PHEV) is equipped with a large-capacity power battery pack. On the one hand,

it can replenish energy from the grid and has a long driving range [4], [5]. On the other hand, it can recover more braking energy and has excellent fuel economy [6]. Moreover, PHEV can also be connected to the grid through vehicle-to-grid, which will facilitate the implementation of energy saving and emission reduction and ensure the more flexible use of vehicle batteries [7], [8]. Therefore, the PHEV is becoming more and more popular. However, the battery needs to be frequently charged and discharged to meet the vehicle's power requirements, which will inevitably accelerate battery aging [9]. At present, power batteries are expensive and have not achieved a breakthrough in cycle life [10]. Battery aging costs account for a large part of vehicle operating costs. Therefore, how to maximize the service life of the battery is the key to solve the battery problem.

Compared with the battery, the supercapacitor (SC) has much higher power density and cycle life [11], but lower energy density [12]. Combining SCs and batteries to form a hybrid energy storage system (HESS) can give full play to their advantages, and can effectively slow down the aging rate of batteries [13], [14]. When the HESS is applied to a PHEV, the braking energy can be stored both in the SC and the battery. The energy stored in the SC can be used to accelerate the vehicle, while the energy stored in the battery can be used to provide smooth power requirements of the vehicle [15]. Compared with the battery energy storage system (BESS), the HESS have the characteristics of high-power density and high cycle life, which will effectively improve the overall performance of the vehicle. The use of HESSs in regenerative braking energy recovery on urban traffic vehicles is more economical and common [16]. The application of HESSs faces two major challenges, one is how to have a longer service life, and the other is how to design a smaller size. To solve these problems, the energy management strategy (EMS) and size of the HESS need to be optimized.

### A. ENERGY STORAGE UNIT LIFE MODEL

The establishment of the energy storage unit (ESU) life model has always been a research hotspot and difficulty. Many scholars have studied the mechanism of battery performance degradation, and given the corresponding battery life degradation model. Song *et al.* [17] proposed a novel battery degradation model which was effective in a wide temperature range. Li et al [14] developed a cycle life model to predict the battery cycle ability accurately. At present, there are few studies on the lifetime degradation model of the SC. In this paper, a simple but efficient model of battery and SC life degradation is established, which can quantify the aging of the ESU online and provide a basis for subsequent power optimization and size optimization of the HESS.

### B. ENERGY MANAGEMENT STRATEGY

The EMS is the core of the hybrid power system, which determines the power, stability and economy of the vehicle [18]. In recent years, various algorithms have been developed and applied to PHEV energy management. These energy management methods can be divided into two categories, namely rule-based methods and optimization-based methods [19]. Rule-based energy management methods are obtained based on experience, including the definite rule EMS and the fuzzy rule EMS. With the development of intelligent algorithms, some advanced algorithms including dynamic programming (DP) [20], [21], convex programming [22], model predictive control (MPC) [23], [24], particle swarm optimization (PSO) [25] and reinforcement learning (RL) [26] are applied to hybrid electric vehicle energy management. Song et al [27] compared four semi-active hybrid energy storage system topologies and proposed on-line control strategies related to different topologies. Another good study from the same research group [28] proposed a soft-run strategy for real-time and multi-objective control algorithm design. Du et al [29] proposed an algorithm based on two-dimensional Pontryagin's minimum principle to distribute power for PHEV with multi-energy storage system, and simulation results showed that the total vehicle operating cost was significantly reduced compared to the PHEV with BESS. DP approach [30], [31] has been employed to develop optimal control strategy for the HESS in a PHEV. Compared with the rule-based method, these optimization-based methods can further improve the vehicle's power and economic performance. In the open literature, the DP algorithm is the most widely used. It can obtain global optimal results, and is often used as a benchmark for comparing the performance of other algorithms. The EMS of the PHEV with a HESS needs to consider the characteristics of each ESU. Therefore, compared to vehicles with a single energy storage system, the formulation of a power distribution strategy is more complicated. However, few EMSs both consider ESU aging and fuel economy of the vehicle. In order to simultaneously optimize the vehicle's fuel economy and ESU service life, this paper proposes a hierarchical energy management strategy (HEMS) for power distribution of a PHEV with the HESS. The upper layer uses a DP algorithm to coordinate the power distribution between the engine and the motor to optimize vehicle fuel consumption. The lower layer establishes a kind of linear programming model considering battery life degradation to allocate the power of the HESS.

### C. SIZE OPTIMIZATION METHOD

The HESS in a PHEV can take advantage of the high energy density of the battery and the high power density of the SC [32]. The HESS has a corresponding optimal size in every common scenario. A reasonable size can not only give full play to the performance of each ESU, but also reduce the cost of the system [33]. Many scholars have done innovative research to optimize the size of the HESS. Ref [34] has found the optimal capacity of the battery and the SC based on the Pontryagin's minimum principle. Ref [35] has optimized the size of the HESS in electric vehicles based on genetic algorithm. In Ref [36], a methodology based on the statistical description of driving cycles has been proposed to optimize the size of the energy source of a hybrid vehicle. In Ref [37], a multi-objective optimization method focused on minimizing system cost, weight, and volume has been

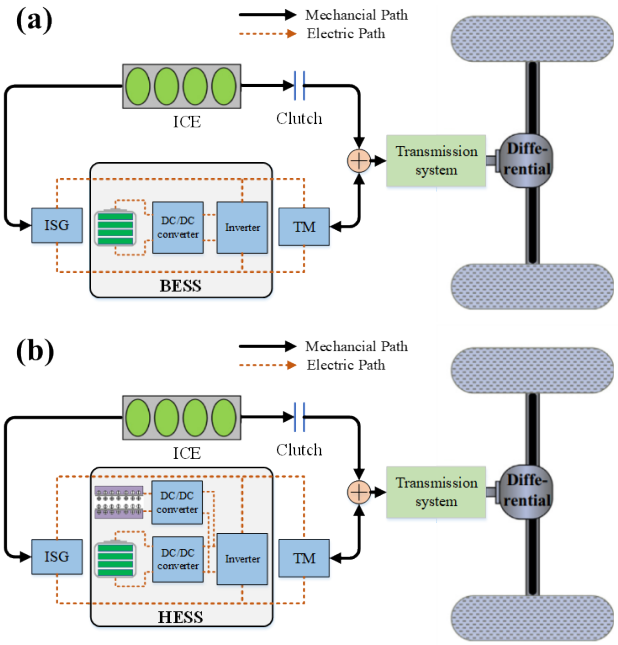


**FIGURE 1.** Topology of different PHEV powertrains: (a) The series-parallel powertrain with a BESS; (b) The series-parallel powertrain with a HESS.

investigated to optimally size a battery unit and supercapacitor hybrid energy storage system for PHEV. However, few size optimization methods can simultaneously optimize the power and capacity of each ESU while extending battery life. This paper proposes a multi-dimensional size optimization framework, which is different from existing researches. It can simultaneously determine the maximum power of the system, the maximum power and capacity of the battery, and the maximum power and capacity of the SC under the constraints of power and energy requirements and battery life decay rate.

In order to give full play to the performance of the energy storage system and reduce the total operating cost of the vehicle, this paper optimizes the power and size of the HESS in a PHEV. The main contributions are summarized as follows:

(1) A size optimization framework is proposed to find the optimal configuration of the HESS, including the maximum power of the system, the maximum power and capacity of the battery, and the maximum power and capacity of the SC.

(2) A HEMS is proposed to simultaneously optimize vehicle fuel economy and battery service life.

(3) Models of battery and SC life degradation are proposed to quantify their life aging in real time.

The rest of the paper is organized as follows: Section II briefly introduces the system configuration, the PHEV modeling and the ESU life degradation model. The overall simulation methodology is presented in Section III. Section IV investigates the power optimization methodology. Size optimization methodology is described in Section V. Section VI discusses the simulation results. Conclusions are provided in Section VII.

**TABLE 1.** Main parameters of the PHEV.

| Component | Parameter | value |
|---|---|---|
| ICE | Maximum power/kW | 147 |
| | Maximum torque/Nm | 804 |
| | Maximum speed/rpm | 2600 |
| ISG | Maximum power/kW | 55 |
| | Maximum torque/N | 500 |
| TM | Maximum power/kW | 168 |
| | Maximum torque/N | 2000 |
| Battery | Capacity/kWh | 34.56 |
| | Voltage/V | 576 |
| Vehicle | Curb weight/kg | 18000 |
| | Frontal area/$m^2$ | 6.6 |
| | Air resistance coefficient | 0.55 |
| | Rolling resistance coefficient | 0.0095 |

## II. MODELING

### A. SYSTEM CONFIGURATION

As shown in Fig. 1 (a), the topology of a typical series-parallel PHEV is mainly composed of a conventional internal combustion engine (ICE), an integrated starter generator (ISG), a traction motor (TM), a transmission system, an automatically controllable friction clutch, and a BESS. In Ref. [12], [20], [38], this configuration has been studied in detail, and its specific parameters are shown in Table 1. Compared with the series and the parallel powertrains, the series-parallel powertrain has more driving modes, and the ICE and the TM can independently deliver power to the wheels. As shown in Fig. 1 (b), in order to effectively extend the battery life, this paper uses a HESS to replace the BESS in a typical PHEV. The topology of the HESS is parallel and fully active. The battery and the SC in this configuration can be controlled independently, which can effectively increase the flexibility of the system [9]. In this power, note that B-PHEV is the abbreviation for the typical series-parallel PHEV. Note the H-PHEV is the abbreviation for the series-parallel PHEV with a HESS.

In this paper, B-PHEV is used as a benchmark to evaluate the size-optimized and power-optimized performance of H-PHEV.

### B. PHEV MODELING

#### 1) THE ICE MODEL

The ICE model is developed based on the engine steady-state test data, assuming that the engine has been fully warmed up, ignoring the effect of engine temperature on fuel consumption rate. The engine is tested at different throttle openings to obtain steady-state output speed, torque and fuel consumption data at different speeds. Then based on the interpolation fitting, the 3-D MAP of the fuel consumption rate with respect to the engine speed and torque can be obtained as shown in Fig.2. The ICE fuel consumption rate $b_e$(g/(kWh)) is an interpolates function of the ICE speed $n_e$(rpm) and torque $T_e$(Nm), which can be presented as follows:

$$b_e(n_e, T_e) = f\,(n_e, T_e) \tag{1}$$

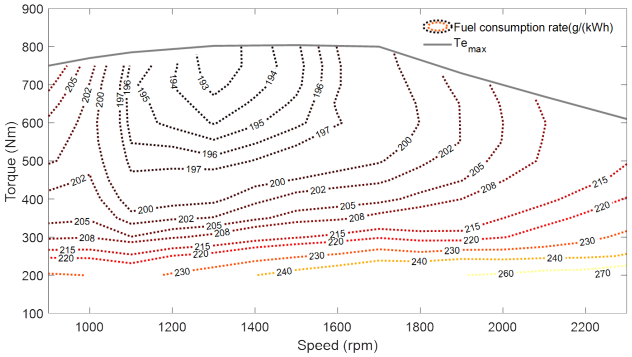


**FIGURE 2.** The ICE fuel consumption map.

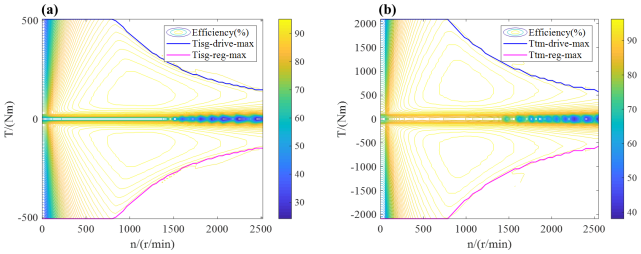


**FIGURE 3.** (a) The ISG efficiency map; (b) The TM efficiency map.

The ICE fuel consumption can be calculated as follows:

$$V_e = \frac{\int T_e \cdot n_e \cdot b_e dt}{9550 \cdot 3600 \cdot \rho_{fuel}} \tag{2}$$

where, $V_e$(L) is the ICE fuel consumption; $\rho_{fuel}$(g/L) is the fuel density.

### 2) ISG and TM models

Experimental modeling methods are also used to establish the ISG model and the TM model. The efficiency, torque and speed data of the motor are obtained based on the experimental, then the nonlinear function relationship between them is obtained by fitting the interpolation function. Finally, ISG and TM efficiency maps can be obtained, which are shown in Fig. 3(a) and Fig. 3(b), respectively. The motor efficiency $\eta_m$ is an interpolates function of the motor outputs speed $n_m$(rpm) and torque $T_m$(Nm), which can be formulated as follows:

$$\eta_m (n_m, T_m) = f (n_m, T_m) \tag{3}$$

### 3) THE ESS MODEL

Ignoring the complex chemical reactions inside the ESS, a linear ESS model is established in this paper. The state of energy (SOE) is selected as the state variable, and its first derivative with respect to time can be expressed as follows:

$$\frac{dSOE}{dt} = -\frac{P_{ESS}}{3600 \cdot E_{ESS}} \tag{4}$$

where, $P_{ESS}$(kW) is the operating power of the ESS; $E_{ESS}$(kWh) is the capacity of the ESS.

### 4) THE VEHICLE MODEL

In the longitudinal direction, the driving force $F_d$(N) provided by the power system needs to overcome rolling resistance $F_f$(N), aerodynamic drag $F_w$(N), climbing resistance $F_i$(N) and acceleration resistance $F_a$(N) to drive the vehicle to the target direction. Therefore, the vehicle longitudinal dynamics model can be formulated as follows:

$$\begin{aligned} F_d &= F_f + F_w + F_i + F_a \\ &= mgf\cos\alpha + \frac{1}{2}C_D A\rho_{air}v^2 + mg\sin\alpha + \delta m\frac{dv}{dt} \end{aligned} \tag{5}$$

where, $m$(kg) is the vehicle curb weight; $g$(m/s$^2$) is the gravitational acceleration; $f$ is the rolling resistance coefficient; $\alpha$ is the road gradient; $C_D$ is the air resistance coefficient; $A$(m$^2$) is the frontal area; $\rho_{air}$(kg/m$^3$) is the air density; $v$(m/s) is the vehicle velocity; $\delta$ is the mass factor that equivalently converts the rotational inertias of rotating components into translational mass; $dv/dt$(m/s$^2$) is the driving acceleration.

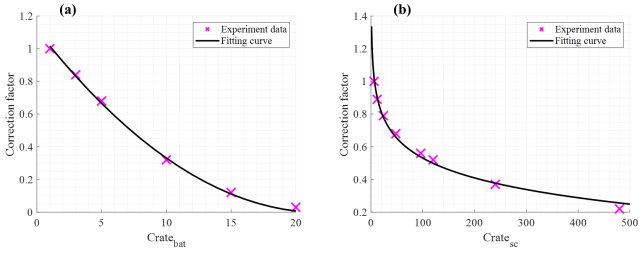


**FIGURE 4.** ESU cycle life correction factor vs. Crate: (a) Battery; (b) SC.

## C. ENERGY STORAGE UNIT LIFE DEGRADATION MODEL

The ESU is considered to reach the end of its life when 20% of capacity has been lost. In the life cycle, the battery can work 5000 full cycles [39], and the SC can work 100,000 full cycles. The life of the ESU is also affected by the charge/discharge rate (Crate). Fig. 4(a) shows the relationship between the battery's cycle life correction factor and Crate [40]. The best fitting result is presented in Eq. (6). Fig. 4(b) shows the relationship between the SC's cycle life correction factor and Crate. The best fitting result is presented in Eq. (7).

$$CF_{bat}\,(Crate) = a \cdot Crate^2 + b \cdot Crate + c \tag{6}$$

$$CF_{sc}\,(Crate) = d \cdot \ln\,(Crate) + e \tag{7}$$

where $a, b, c, d, e$ are curve-fitting coefficients, and the values are 0.0023, -0.1014, 1.1146, -0.175, 1.3366, respectively.

For each ESU, the total energy it can release during its life cycle is constant. Therefore, the life degradation factor of a battery and a SC can be formulated as Eq. (8) and Eq. (9), respectively.

$$\eta_{bat} = \frac{\int P_{bat}^{dis} \cdot CF_{bat}^{-1} dt}{5000 \cdot 3600 \cdot E_{bat}} \tag{8}$$

$$\eta_{sc} = \frac{\int P_{sc}^{dis} \cdot CF_{sc}^{-1} dt}{100000 \cdot 3600 \cdot E_{sc}} \tag{9}$$

where, $P_{bat}^{dis}$(kW) and $P_{sc}^{dis}$(kW) are the discharge power during battery and SC operation, respectively; $E_{bat}$(kWh) and $E_{sc}$(kWh) are the capacity of the battery and the SC, respectively.

## III. SIMULATION METHODOLOGY

For B-PHEV, in order to effectively reduce the vehicle operating cost, the power between the engine and the motor needs to be optimized. As for H-PHEV, it is also necessary to optimize the size and power distribution of the HESS. The overall simulation methodology of this paper is shown in Fig.5.

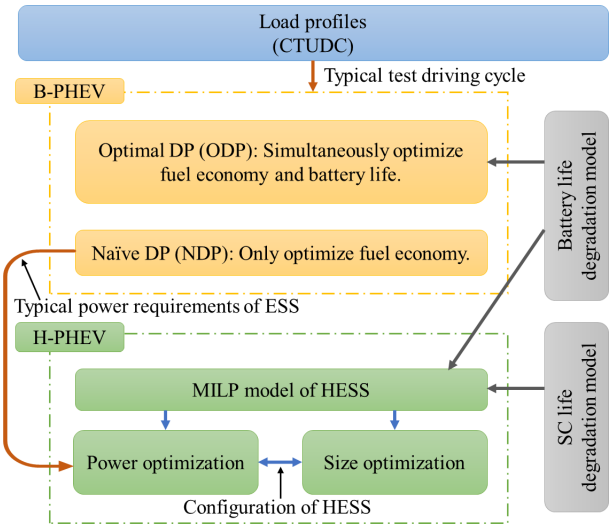


**FIGURE 5.** Overall simulation methodology.

The simulation methodology can be divided into the following three parts:

### 1) OPTIMAL DP

Aiming at B-PHEV, based on DP algorithm and using battery life degradation model, this paper develops a power distribution strategy with vehicle fuel consumption and battery aging cost as multi-objective functions. This method is called optimal DP (ODP), which can simultaneously optimize the vehicle's fuel economy and battery service life.

### 2) HEMS

At the upper level, the naïve DP (NDP) strategy with the vehicle fuel economy as the optimization goal is used to complete the power distribution between the engine and the motor in the B-PHEV, so as to obtain the typical power demand of the energy storage system. At the lower level, a HESS is used to replace the BESS, and then combined with the battery and SC life degradation model, a kind of linear programming model of the HESS is established.

### 3) SIZE OPTIMIZATION

Numerical model of HESS is developed based on a kind of linear optimization. It takes the typical power requirements of the energy storage system as input and aims at the lowest annual operating cost of the system to optimize the configuration of the HESS including the maximum power of the system, the maximum power and capacity of the battery, and the maximum power and capacity of the SC.

The simulation is performed on Matlab/Simulink platform. And it takes an average of 8 hours to complete one such simulation of size optimization and power optimization using a computer with an Inter Core i7-8550U 1.99GHz processor, 8GB of RAM and 64-bit Windows operating system.

## IV. POWER OPTIMIZATION METHODOLOGY

This paper studies and compares two PHEV powertrain topologies: B-PHEV and H-PHEV. Two energy management strategies are applied to B-PHEV, they are NDP strategy and ODP strategy. As for H-PHEV, a HEMS is proposed in this paper. At the upper layer, the NDP strategy is used to coordinate the power distribution between the ICE and the motor to obtain the typical power requirements of the energy storage system, which can ensure the optimal fuel economy of the vehicle. In the lower layer, taking the power requirements of the energy storage system as input, the optimisation method considering ESU life degradation is introduced to allocate power between the battery and the SC.

### A. NDP STRATEGY AND ODP STRATEGY

DP is a global optimization algorithm based on Bellman's principle, which divides the entire optimization problem into a series of sub-solving problems with discrete steps [41]. With a thorough search of all state and control grids under consideration of constraints, the controlled system minimizes the cost function in the process of state variable migration, thereby obtaining a theoretically optimal control sequence.

For B-PHEV, the ODP strategy can simultaneously optimize vehicle fuel economy and battery service life. In HEMS, the NDP strategy is used in the upper-layer optimization. It obtains the typical power requirements of the energy storage system by allocating the power between the motor and the engine of B-PHEV to ensure the optimal fuel economy of the vehicle. Both NDP and ODP strategies are developed based on the DP algorithm. Their constraints and state transfer function are the same, but the objective function is different.

First, the SOE of the BESS is selected as the state variable of the system. ICE torque $T_e$, ISG torque $T_{isg}$, TM torque $T_{tm}$, clutch state $S_{clu}$ and braking torque $T_b$ are selected as the control variables of the system.

The series-parallel powertrain can be described as discrete controlled system, and the process of state transition can be presented as follows:

$$x_{k+1} = f_k\left(x_k, u_k\right) \tag{10}$$

where, $f_k$ is the state transition function; $x_k$ is the state variable of the system; $u_k$ is the control variable of the system.

The NDP strategy only optimizes the vehicle's fuel economy and ensures that the vehicle's fuel consumption is minimal. The ODP strategy simultaneously optimizes the vehicle's fuel economy and battery service life, and finds

the optimal solution through the confrontation of these two optimization goals.

The remaining cost function $J$ of the system from time $k$ to time $N$ is formulated as follows:

$$L(x_i, u_i) = \begin{cases} L_{NDP}(x_i, u_i) = L_{fuel}(x_i, u_i) \\ L_{ODP}(x_i, u_i) = L_{fuel}(x_i, u_i) + L_{loss}(x_i, u_i) \end{cases} \tag{11}$$

$$J(x_k) = \sum_{i=k}^{N} L(x_i, u_i) \tag{12}$$

where, $L(x_i, u_i)$ is the instantaneous cost function at time $i$.

At any time, the optimal control sequence $\pi_i = (u_{i+1}, u_{i+2}, \cdots, u_N)$ minimizes the residual cost function $J$ of the system. Therefore, the optimization problem at time $k$ can be transformed into the following formula:

$$\min(J(x_k)) = \min(L(x_k, u_k) + J(x_{k+1})) \tag{13}$$

where, $J(x_{k+1})$ is the remaining cost of the system from time $k+1$ to time $N$.

To ensure that the system operates smoothly and safely, the components of the series-parallel powertrain need to be restrained as follows:

$$\begin{cases} SOE_{BESS}^{\min} \le SOE_{BESS}^{k} \le SOE_{BESS}^{\max} \\ n_e^{\min} \le n_e^k \le n_e^{\max} \\ T_e^{\min}\left(n_e^k\right) \le T_e^k \le T_e^{\max}\left(n_e^k\right) \\ n_{isg}^{\min} \le n_{isg}^k \le n_{isg}^{\max} \\ T_{isg}^{\min}\left(n_{isg}^k, SOE_{ESS}^k\right) \le T_{isg}^k \le T_{isg}^{\max}\left(n_{isg}^k, SOE_{ESS}^k\right) \\ n_{tm}^{\min} \le n_{tm}^k \le n_{tm}^{\max} \\ T_{tm}^{\min}\left(n_{tm}^k, SOE_{ESS}^k\right) \le T_{tm}^k \le T_{tm}^{\max}\left(n_{tm}^k, SOE_{ESS}^k\right) \\ T_d^k = T_e^k + T_{isg}^k + T_{tm}^k + T_b^k / i_0 \\ n_{tm}^k = n_e^k = n_{isg}^k \, if \; clutch = 1 \\ T_{isg}^k = n_{isg}^k \, if \; clutch = 0 \\ T_e^k + T_{isg}^k = 0 \; if \; clutch = 0 \end{cases} \tag{14}$$

where, $n_e^k, n_{isg}^k, n_{tm}^k$ are the speed of ICE, ISG, and TM at time $k$, respectively. $T_e^k, T_{isg}^k, T_{tm}^k$ are the torques of ICE, ISG and TM at time $k$, respectively. $T_b^k$ is the hydraulic brake torque at time $k$. $T_d^k$ is the vehicle torque demand at time $k$; $i_0$ is the ratio of the final gear; $clutch = 1$ means the clutch is in the closed state; $clutch = 0$ means the clutch is in the released state.

### B. NUMERICAL CONSTRAINTS

The BESS is limited to a low cycle life, and the vehicle's braking energy recovery will accelerate battery aging. In order to ensure vehicle fuel economy and effectively suppress battery aging, a HESS is used to replace the BESS. SC has the characteristics of high-power density and high cycle life. By working together with the battery, they can not only ensure the vehicle's fuel economy of but also extend the battery life. In HEMS, the power of the energy storage system obtained by the upper layer optimization is used as the input of the lower layer optimization. At the lower level, a multi-objective optimization model is established to distribute the power of the battery and the SC in the HESS.

The linear programming method has high calculation efficiency [42]. The SOE of the battery and the SC are selected as the state variables of the system. At any time, they need to be constrained as follows:

$$\begin{cases} SOE_{bat}^{\min} \le SOE_{bat}^{i} \le SOE_{bat}^{\max} \\ SOE_{sc}^{\min} \le SOE_{sc}^{i} \le SOE_{sc}^{\max} \end{cases} \tag{15}$$

where, $SOE_{bat}^i$ and $SOE_{sc}^i$ are the SOE of the battery and the SC at time $i$, respectively.

To ensure the safe operation of the battery and the SC, their charge and discharge power needs to be constrained at any time as follows:

$$\begin{cases} P_{batc}^{\min} \cdot S_{batc}^i \le P_{batc}^i < 0 \\ 0 \le P_{batd}^i \le P_{batd}^{\max} \cdot S_{batd}^i \\ P_{scc}^{\min} \cdot S_{scc}^i \le P_{scc}^i < 0 \\ 0 \le P_{scd}^i \le P_{scd}^{\max} \cdot S_{scd}^i \end{cases} \tag{16}$$

where, $P_{batc}^i$ and $P_{scc}^i$ are the charging power of the battery and the SC, respectively; $P_{batd}^i$ and $P_{scd}^i$ are the discharging power of the battery and the SC, respectively; $S_{batc}^i, S_{scc}^i, S_{batd}^i$ and $S_{scd}^i$ are 0-1 variables, which indicate whether the battery and the SC are charged or discharged at time $i$, respectively.

The charge and discharge states of the battery and the SC are unique at the same time, which can be shown as follows:

$$\begin{cases} S_{batc}^i + S_{batd}^i \le 1 \\ S_{scc}^i + S_{scd}^i \le 1 \end{cases} \tag{17}$$

The sum of the power of the battery and the SC must always meet the power requirements $P_{ESS}^i$ of the ESS, which can be demonstrated as follows:

$$P_{ESS}^i = P_{batc}^i + P_{batd}^i + P_{scc}^i + P_{scd}^i \tag{18}$$

In the HESS, the battery's cycle life is much smaller than that of the SC, and it is greatly affected by the charge and discharge rate. Therefore, in the power distribution process, a constraint is imposed on the battery's power change rate, which can be formulated as follows:

$$\begin{cases} R_{ESS}^i = P_{ESS}^i - P_{ESS}^{i-1} \\ P_{batc}^i + P_{batd}^i - \left(P_{batc}^{i-1} + P_{batd}^{i-1}\right) \le R_{ESS}^i \end{cases} \tag{19}$$

where, $R_{ESS}^i$ is the power change rate of the ESS.

The battery's cycle life is also affected by the number of charge and discharge cycles. The restrictions on the number of charge and discharge times of the battery in the power distribution process are as follows:

$$\sum_{i=2}^{N} \left| S_{batc}^i - S_{batc}^{i-1} \right| \le Q \text{ or } \sum_{i=2}^{N} \left| S_{batd}^i - S_{batd}^{i-1} \right| \le Q \tag{20}$$

where, $Q$ is the set maximum battery charge and discharge times.

Combined with the ESU life degradation model, the power distribution of the HESS is completed with the minimum degradation of system life, which can be shown as follows:

$$Z_{power} = \min\left(\eta_{bat} \cdot C_{bat} + \eta_{sc} \cdot C_{sc}\right) \tag{21}$$

where, $C_{bat}$ and $C_{sc}$ are the initial costs of the battery and the SC, respectively.

## V. SIZE OPTIMIZATION METHODOLOGY

As the size of an ESS increases, its life degradation factor will decrease, but the cost of the system will increase. Therefore, in order to make full use of the performance of each ESU, it is necessary to find an optimization point between system cost and system size.

**TABLE 2. The multi-dimensional size optimization framework.**

**Algorithm:** Size optimization

**Input:** Typical demand power of the HESS
**Output:** Optimal configuration of the HESS
1: Select optimization variables: the maximum power standard value of the battery $P_{bat}^{\max}$, the maximum power standard value of the HESS $P_{HESS}^{\max}$, the maximum Crate of the battery $Crate_{bat}^{\max}$, and the maximum Crate of the SC $Crate_{sc}^{\max}$
2: **for** $P_{HESS}^{\max} \leftarrow P_{HESS}^{\max}(1)$ to $P_{HESS}^{\max}(k)$ **do**
3: **for** $P_{bat}^{\max} \leftarrow P_{bat}^{\max}(1)$ to $P_{bat}^{\max}(m)$ **do**
4: **for** $Crate_{bat}^{\max} \leftarrow Crate_{bat}^{\max}(1)$ to $Crate_{bat}^{\max}(n)$ **do**
5: **for** $Crate_{sc}^{\max} \leftarrow Crate_{sc}^{\max}(1)$ to $Crate_{sc}^{\max}(s)$ **do**
6: Convert the demand power of the HESS into standard values
7: $P_{sc}^{\max} \leftarrow |\ P_{HESS}^{\max} - P_{bat}^{\max}\ |$
8: Optimal power allocation based on the linear programming
9: Record the total annual operating cost of the system
10: **end for**
11: **end for**
12: **end for**
13: **end for**
14: Select the configuration with the lowest annual operating cost

In this paper, a multi-dimensional size optimization framework is proposed. As shown in Table 2, this method takes the typical power data of the ESS as input, and finds the optimal configuration of the system, including the maximum power of the system, the maximum power and capacity of the battery, and the maximum power and capacity of the SC. The size optimization framework takes the typical power requirements of the HESS as input, and finds the optimal configuration of the HESS through discrete optimization of various optimization parameters. The proposed power distribution approach and size optimization approach can be potentially used in the other applications, for example a microgrid system with HESS. For different application scenarios, the typical power requirements of the system are used as input, and the constraints are changed based on the operating characteristics of the system.

The size optimization method finds the ESS configuration that minimizes the annual operating cost of the system by comprehensively considering the life degradation cost of each ESU, the power converter cost $C_{convert}$, and the system thermal management cost $C_{thermal}$. The objective function for size optimization can be formulated as follows:

$$Z_{size} = \min\left(\beta \cdot Z_{power} + \frac{1}{L}\left(C_{convert} + C_{thermal}\right)\right) \tag{22}$$

where, $\beta$ is the annual operating cost coefficient of the system; $L$(year) is the design service life of the system.

The process of solving the optimal configuration of the HESS can be divided into the following steps:

First, the maximum power standard value of the system, the maximum power standard value of the battery, the maximum Crate of the battery and the maximum Crate of the SC are selected as optimization variables.

Second, standardize the required power of the ESS and give each optimization variable a range. Then, for each configuration, the power is optimally allocated based on the optimization model, and the annual operating cost of the system is recorded.

Finally, the configuration with the lowest annual operating cost is selected as a result of the size optimization. Based on the value of each optimization variable, the peak power of the system, the maximum power and capacity of the battery, and the maximum power and capacity of the SC can be obtained.

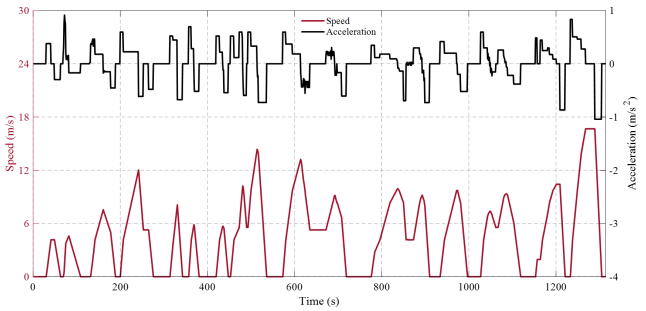


**FIGURE 6. The velocity and acceleration profile of CTUDC cycle.**

## VI. SIMULATION RESULTS AND DISCUSSION

The PHEV studied in this paper is a bus driving on urban roads, so the Chinese typical urban driving cycle (CTUDC) is selected as the test driving cycle. As shown in Fig. 6, CTUDC has a driving distance of 5.897km and a driving time of 1314 seconds. The capacity price of the battery is 600 \$/kWh, and the capacity price of the SC is 3600 \$/kWh [39].

Focusing on the B-PHEV, the NDP and ODP strategies are applied to the ICE and the motor power distribution process. The simulation results are shown in Fig. 7. When the battery life degradation is considered in the EMS, the proportion of the battery's charging power is greatly reduced, and the SOE curve of the battery changes more smoothly. This shows that the battery does not need to directly obtain energy from regenerative braking, so frequent charging and discharging are avoided, which will effectively extend the

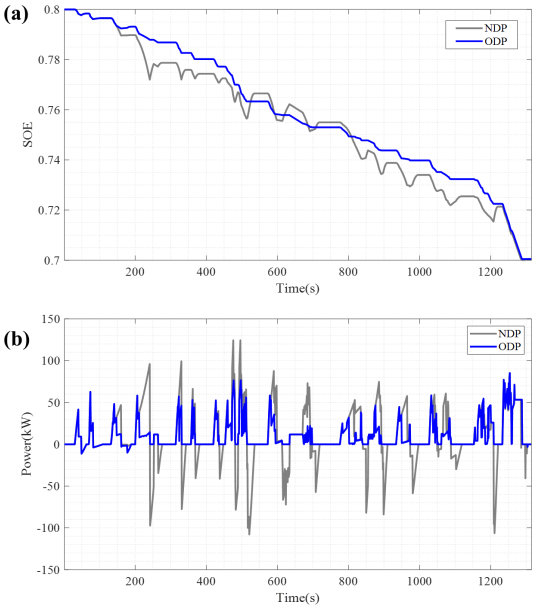


**FIGURE 7.** (a) Comparison of battery SOE between two EMSs; (b) Comparison of battery power between two EMSs.

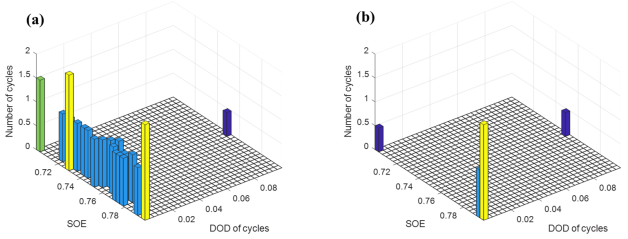


**FIGURE 8.** Number and depth of battery charge and discharge cycles: (a) NDP; (b) ODP.

battery life. When battery life degradation is not considered in the EMS, the battery recovers as much braking energy as possible to improve fuel economy. Based on these results, it can be concluded that the currently used EMSs focus on improving the recovery of braking energy, but is not friendly to the protection of battery life.

In order to quantify the effect of prolonging the battery life, this paper introduces a rain-flow counting algorithm, which is used to calculate the number of charge and discharge cycles and the depth of charge and discharge (DOD) of each cycle [7], [12], [43]. As shown in Fig. 8, when DP does not consider battery life degradation, the number of battery charge and discharge cycles is 22. When DP considers battery life degradation, the number of battery charge and discharge cycles is 4. Obviously, the number of charge and discharge cycles of the battery is significantly reduced, which will effectively extend the battery life.

As for the H-PHEV, this paper proposes a HEMS and a multi-dimensional size optimization framework. In the upper layer optimization, NDP strategy is used to optimize the power distribution of the ICE and the motor. The lower layer optimization bases on the CPLEX solver [44], and is used to optimize the battery and the SC power distribution. Then, based on the typical power of the ESS obtained by the DP algorithm, the size of the ESS is optimized using a multi-dimensional size optimization framework. During the simulation process, the set life of the PHEV is 10 years, it operates 12 CTUDCs every day, and runs 300 days per year. The thermal management price of the ESS is 80$/kWh, and the price of the power converter is 50$/kW [40].

**TABLE 3.** Comparison of size optimization results for the HESS with different maximum power.

| Parameters | BESS | HESS (a) | HESS (b) | HESS (c) |
|---|---|---|---|---|
| Battery maximum power (kW) | 125 | 50 | 37.5 | 50 |
| SC maximum power (kW) | / | 75 | 100 | 100 |
| Battery capacity (kWh) | 34.56 | 25 | 18.75 | 16.7 |
| SC capacity (kWh) | / | 3.75 | 5 | 5 |
| System maximum power (kW) | 125 | 125 | 137.5 | 150 |
| System capacity (kWh) | 34.56 | 28.75 | 23.75 | 21.7 |
| Battery aging cost ($/year) | 2388 | 927 | 665 | 662 |
| SC aging cost ($/year) | / | 409 | 484 | 487 |
| Convert cost ($/year) | 625 | 625 | 687.5 | 750 |
| Thermal management cost ($/year) | 276.5 | 230 | 190 | 173.6 |
| ESS total cost ($/year) | 3289.5 | 2191 | 2026.5 | 2072.6 |
| System capacity (%) | 100 | 83.2 | 68.7 | 62.8 |
| ESS total economy (%) | 100 | 66.6 | 61.6 | 63 |

The optimal results of HESS sizes with different maximum powers are shown in Table 3. When the maximum power standard value of the system is 1.1, the economy of the system is the best, so the configuration of HESS (b) is the result of size optimization. Compared with BESS, the total capacity of HESS (b) is reduced by 31.3%, and the overall economy is improved by 37.8%. This fully proves that after size optimization, HESS is more economical and smaller in size.

The upper layer of the HEMS optimizes the vehicle's fuel economy, and the lower layer minimizes the life degradation of the ESS. The result of the power distribution of the HESS is shown in Fig. 9 (a). The SC recovers regenerative braking energy. The battery rarely obtains energy from regenerative braking, which makes the battery avoid frequent charging and discharging. As shown in Fig. 9 (b), the change of battery SOE is gentle. As shown in Fig. 9 (c), based on the calculation of the rain-flow counting algorithm, the number of battery charge and discharge cycles is 2.5. Compared with the two EMSs applied to B-PHEV, the effect of battery aging suppression is significantly improved.

As shown in Fig. 10, for the B-PHEV, when the DP algorithm only focuses on improving fuel economy, the battery life degradation rate after operating a CTUDC is 3.2046e-05. When the DP algorithm optimizes both fuel economy and battery life degradation rate, the battery life degradation rate after operating a CTUDC is 1.9684e-05. When H-PHEV is the research goal, the optimal configuration of the HESS is first obtained based on the size optimization framework, and then the vehicle power is optimized using HEMS. The simulation results show that the battery life degradation rate after

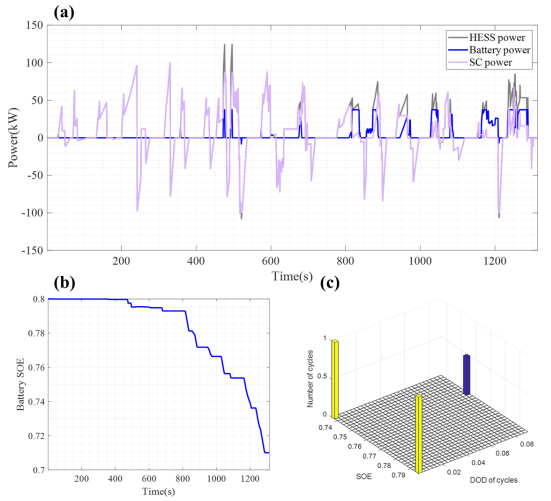


**FIGURE 9.** Simulation results of the HEMS: (a) Power distribution results; (b) Battery SOE; (c) Number and depth of battery charge and discharge cycles.

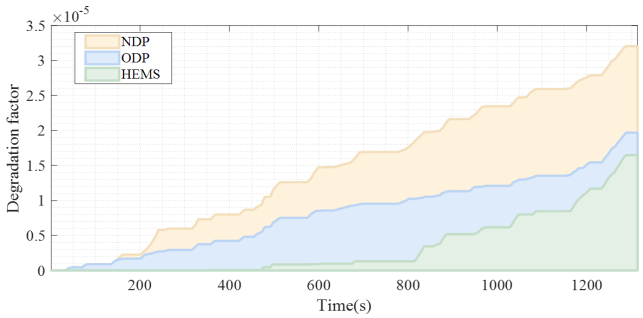


**FIGURE 10.** Battery life degradation rate vs. time under three energy management strategies.

operating a CTUDC is 1.6471e-05. This fully demonstrates the advantages of the size optimization method and HEMS proposed in this paper.

**TABLE 4.** Comparison of annual operating costs of the vehicle under different powertrain topologies and different EMSs.

| Parameters | B-PHEV | | H-PHEV |
|---|---|---|---|
| EMS | NDP | ODP | HEMS |
| ESS loss cost ($/year) | 3289.5 | 2368.5 | 2026.5 |
| Fuel cost ($/year) | 1654.4 | 1941.6 | 1654.4 |
| Electricity cost ($/year) | 1307.7 | 1307.7 | 1307.7 |
| Total cost ($/year) | 6251.6 | 5617.8 | 4988.6 |
| Battery aging (%) | 100 | 61.6 | 51.6 |
| Total economy (%) | 100 | 89.9 | 79.8 |

The details of the annual operating cost of vehicles with different powertrain topologies and different EMSs are listed in Table 4. The economic results obtained by applying the NDP strategy to the B-PHEV serve as a benchmark for comparison. When the ODP strategy is applied to B-PHEV energy management, the simulation results show that the aging cost of the battery is reduced by 38.4%, but fuel consumption is increased by 17.4% compared to the benchmark. This is because in order to suppress battery aging, the recovery of regenerative braking energy by the battery is greatly reduced. As for H-PHEV, the optimal configuration of the HESS is first obtained based on the size optimization framework, and then the vehicle power is optimized using HEMS. The simulation results show that compared with the benchmark, the vehicle's fuel consumption has not increased, but the battery aging cost has been reduced by 48.9%, and the total cost has been reduced by 21.2%. Therefore, it can be concluded that the size optimization framework and power optimization method of the HESS proposed in this paper are advanced and effective.

## VII. CONCLUSION

This paper optimizes the component size and power of the H-PHEV. The B-PHEV is used as a reference to evaluate the performance of size optimization and power optimization. DP algorithm that only optimizes fuel economy is set as a benchmark for comparison.

First, this paper establishes a life degradation model of the ESU. Focusing on the B-PHEV, compared to the benchmark, based on the DP algorithm that both optimizes fuel economy and battery life degradation rate, the battery degradation cost is reduced by 38.4%. This proves that the life degradation model of is effective.

To optimize the size of the HESS, this paper proposes a multi-dimensional size optimization framework. When the maximum power of the system is 137.5kW, the maximum power and capacity of the battery are 37.5kW and 18.75kWh respectively, and the maximum power and capacity of the supercapacitor are 100kW and 5kWh respectively, the system has the best economy. Compared with the BESS, the capacity of the system is reduced by 31.3%, and the economy is increased by 37.8%. The size of the system is smaller and the economy is better.

Then, for the H-PHEV power distribution, this paper proposes a HEMS for battery anti-aging. The upper layer uses the DP algorithm to optimize fuel economy, and the lower layer extends battery life. Compared with the benchmark, the battery aging rate has been reduced by 48.9%, and the vehicle economy has increased by 21.2%. This fully demonstrates the advantages of this strategy.

Therefore, it can be concluded that the multi-dimensional size optimization framework and HEMS proposed in this paper can effectively find the optimal configuration of the HESS and extend the battery life.

## REFERENCES

[1] H. Bizhani, G. Yao, S. M. Muyeen, S. M. Islam, and L. Ben-Brahim, "Dual mechanical port machine based hybrid electric vehicle using reduced switch converters," *IEEE Access*, vol. 7, pp. 33665–33676, 2019.
[2] J. Li, R. Xiong, Q. Yang, F. Liang, M. Zhang, and W. Yuan, "Design/test of a hybrid energy storage system for primary frequency control using a dynamic droop method in an isolated microgrid power system," *Appl. Energy*, vol. 201, pp. 257–269, Sep. 2017.
[3] P.-Y. Kong and G. K. Karagiannidis, "Charging schemes for plug-in hybrid electric vehicles in smart grid: A survey," *IEEE Access*, vol. 4, pp. 6846–6875, 2016.
[4] H.-Q. Guo, G. Wei, F. Wang, C. Wang, and S. Du, "Self-learning enhanced energy management for plug-in hybrid electric bus with a target preview based SOC plan method," *IEEE Access*, vol. 7, pp. 103153–103166, 2019.

[5] Z. Chen, N. Guo, J. Shen, R. Xiao, and P. Dong, "A hierarchical energy management strategy for power-split plug-in hybrid electric vehicles considering velocity prediction," *IEEE Access*, vol. 6, pp. 33261–33274, 2018.
[6] Z. Pu, X. Jiao, C. Yang, and S. Fang, "An adaptive stochastic model predictive control strategy for plug-in hybrid electric bus during vehicle-following scenario," *IEEE Access*, vol. 8, pp. 13887–13897, 2020.
[7] S. Li, C. Gu, J. Li, H. Wang, and Q. Yang, "Boosting grid efficiency and resiliency by releasing V2G potentiality through a novel rolling prediction-decision framework and deep-LSTM algorithm," *IEEE Syst. J.*, early access, Jun. 29, 2020, doi: 10.1109/JSYST.2020.3001630.
[8] Y. Li and K. Li, "Incorporating demand response of electric vehicles in scheduling of isolated microgrids with renewables using a bi-level programming approach," *IEEE Access*, vol. 7, pp. 116256–116266, 2019.
[9] J. Cao and A. Emadi, "A new battery/ultracapacitor hybrid energy storage system for electric, hybrid, and plug-in hybrid electric vehicles," *IEEE Trans. Power Electron.*, vol. 27, no. 1, pp. 122–132, Jan. 2012.
[10] M. Faisal, M. A. Hannan, P. J. Ker, A. Hussain, M. B. Mansor, and F. Blaabjerg, "Review of energy storage system technologies in microgrid applications: Issues and challenges," *IEEE Access*, vol. 6, pp. 35143–35164, 2018.
[11] X. Lin and Y. Lei, "Coordinated control strategies for SMES-battery hybrid energy storage systems," *IEEE Access*, vol. 5, pp. 23452–23465, 2017.
[12] Y. Bai, H. He, J. Li, S. Li, Y.-X. Wang, and Q. Yang, "Battery anti-aging control for a plug-in hybrid electric vehicle with a hierarchical optimization energy management strategy," *J. Cleaner Prod.*, vol. 237, Nov. 2019, Art. no. 117841.
[13] C. Wang, B. Huang, and W. Xu, "An integrated energy management strategy with parameter match method for plug-in hybrid electric vehicles," *IEEE Access*, vol. 6, pp. 62204–62214, 2018.
[14] J. Li, R. Xiong, H. Mu, B. Cornélusse, P. Vanderbemden, D. Ernst, and W. Yuan, "Design and real-time test of a hybrid energy storage system in the microgrid with the benefit of improving the battery lifetime," *Appl. Energy*, vol. 218, pp. 470–478, May 2018.
[15] L. Kouchachvili, W. Yaïci, and E. Entchev, "Hybrid battery/supercapacitor energy storage system for the electric vehicles," *J. Power Sources*, vol. 374, pp. 237–248, Jan. 2018.
[16] J. R. Miller, "Engineering electrochemical capacitor applications," *J. Power Sources*, vol. 326, pp. 726–735, Sep. 2016.
[17] Z. Song, H. Hofmann, J. Li, J. Hou, X. Zhang, and M. Ouyang, "The optimization of a hybrid energy storage system at subzero temperatures: Energy management strategy design and battery heating requirement analysis," *Appl. Energy*, vol. 159, pp. 576–588, Dec. 2015.
[18] Z. Amjadi and S. S. Williamson, "Power-electronics-based solutions for plug-in hybrid electric vehicle energy storage and management systems," *IEEE Trans. Ind. Electron.*, vol. 57, no. 2, pp. 608–616, Feb. 2010.
[19] S. G. Wirasingha and A. Emadi, "Classification and review of control strategies for plug-in hybrid electric vehicles," *IEEE Trans. Veh. Technol.*, vol. 60, no. 1, pp. 111–122, Jan. 2011.
[20] J. Li, M. Zhang, Q. Yang, Z. Zhang, and W. Yuan, "SMES/battery hybrid energy storage system for electric buses," *IEEE Trans. Appl. Supercond.*, vol. 26, no. 4, pp. 1–5, Jun. 2016.
[21] W. Wang, Z. Zhang, J. Shi, C. Lin, and Y. Gao, "Optimization of a dual-motor coupled powertrain energy management strategy for a battery electric bus based on dynamic programming method," *IEEE Access*, vol. 6, pp. 32899–32909, 2018.
[22] X. Hu, N. Murgovski, L. M. Johannesson, and B. Egardt, "Optimal dimensioning and power management of a fuel cell/battery hybrid bus via convex programming," *IEEE/ASME Trans. Mechatronics*, vol. 20, no. 1, pp. 457–468, Feb. 2015.
[23] R. T. Bambang, A. S. Rohman, C. J. Dronkers, R. Ortega, and A. Sasongko, "Energy management of fuel cell/battery/supercapacitor hybrid power sources using model predictive control," *IEEE Trans. Ind. Informat.*, vol. 10, no. 4, pp. 1992–2002, 2014.
[24] F. A. Bender, M. Kaszynski, and O. Sawodny, "Drive cycle prediction and energy management optimization for hybrid hydraulic vehicles," *IEEE Trans. Veh. Technol.*, vol. 62, no. 8, pp. 3581–3592, Oct. 2013.
[25] N. Al-Aawar, T. M. Hijazi, and A. A. Arkadan, "Particle swarm optimization of coupled electromechanical systems," *IEEE Trans. Magn.*, vol. 47, no. 5, pp. 1314–1317, May 2011.
[26] J. Wu, H. He, J. Peng, Y. Li, and Z. Li, "Continuous reinforcement learning of energy management with deep q network for a power split hybrid electric bus," *Appl. Energy*, vol. 222, pp. 799–811, Jul. 2018.
[27] Z. Song, H. Hofmann, J. Li, X. Han, X. Zhang, and M. Ouyang, "A comparison study of different semi-active hybrid energy storage system topologies for electric vehicles," *J. Power Sources*, vol. 274, pp. 400–411, Jan. 2015.
[28] Z. Hu, J. Li, L. Xu, Z. Song, C. Fang, M. Ouyang, G. Dou, and G. Kou, "Multi-objective energy management optimization and parameter sizing for proton exchange membrane hybrid fuel cell vehicles," *Energy Convers. Manage.*, vol. 129, pp. 108–121, Dec. 2016.
[29] J. Du, X. Zhang, T. Wang, Z. Song, X. Yang, H. Wang, M. Ouyang, and X. Wu, "Battery degradation minimization oriented energy management strategy for plug-in hybrid electric bus with multi-energy storage system," *Energy*, vol. 165, pp. 153–163, Dec. 2018.
[30] Z. Song, H. Hofmann, J. Li, X. Han, and M. Ouyang, "Optimization for a hybrid energy storage system in electric vehicles using dynamic programing approach," *Appl. Energy*, vol. 139, pp. 151–162, Feb. 2015.
[31] C. Liu, Y. Wang, L. Wang, and Z. Chen, "Load-adaptive real-time energy management strategy for battery/ultracapacitor hybrid energy storage system using dynamic programming optimization," *J. Power Sources*, vol. 438, Oct. 2019, Art. no. 227024.
[32] S. K. Kollimalla, M. K. Mishra, and N. L. Narasamma, "Design and analysis of novel control strategy for battery and supercapacitor storage system," *IEEE Trans. Sustain. Energy*, vol. 5, no. 4, pp. 1137–1144, Oct. 2014.
[33] J. Du, Y. Liu, X. Mo, Y. Li, J. Li, X. Wu, and M. Ouyang, "Impact of high-power charging on the durability and safety of lithium batteries used in long-range battery electric vehicles," *Appl. Energy*, vol. 255, Dec. 2019, Art. no. 113793.
[34] Z. Song, X. Zhang, J. Li, H. Hofmann, M. Ouyang, and J. Du, "Component sizing optimization of plug-in hybrid electric vehicles with the hybrid energy storage system," *Energy*, vol. 144, pp. 393–403, Feb. 2018.
[35] L. Zhang and D. G. Dorrell, "Genetic algorithm based optimal component sizing for an electric vehicle," in *Proc. 39th Annu. Conf. IEEE Ind. Electron. Soc. (IECON)*, Nov. 2013, pp. 7331–7336.
[36] A. Ravey, N. Watrin, B. Blunier, D. Bouquain, and A. Miraoui, "Energy-source-sizing methodology for hybrid fuel cell vehicles based on statistical description of driving cycles," *IEEE Trans. Veh. Technol.*, vol. 60, no. 9, pp. 4164–4174, Nov. 2011.
[37] H. H. Eldeeb, A. T. Elsayed, C. R. Lashway, and O. Mohammed, "Hybrid energy storage sizing and power splitting optimization for plug-in electric vehicles," *IEEE Trans. Ind. Appl.*, vol. 55, no. 3, pp. 2252–2262, May 2019.
[38] J. Li, Q. Yang, F. Robinson, F. Liang, M. Zhang, and W. Yuan, "Design and test of a new droop control algorithm for a SMES/battery hybrid energy storage system," *Energy*, vol. 118, pp. 1110–1122, Jan. 2017.
[39] C. Ju, P. Wang, L. Goel, and Y. Xu, "A two-layer energy management system for microgrids with hybrid energy storage considering degradation costs," *IEEE Trans. Smart Grid*, vol. 9, no. 6, pp. 6047–6057, Nov. 2018.
[40] M. Masih-Tehrani, M.-R. Ha'iri-Yazdi, V. Esfahanian, and A. Safaei, "Optimum sizing and optimum energy management of a hybrid energy storage system for lithium battery life improvement," *J. Power Sources*, vol. 244, pp. 2–10, Dec. 2013.
[41] V. Larsson, L. Johannesson, and B. Egardt, "Analytic solutions to the dynamic programming subproblem in hybrid vehicle energy management," *IEEE Trans. Veh. Technol.*, vol. 64, no. 4, pp. 1458–1467, Apr. 2015.
[42] S. Panuschka and R. Hofmann, "Impact of thermal storage capacity, electricity and emission certificate costs on the optimal operation of an industrial energy system," *Energy Convers. Manage.*, vol. 185, pp. 622–635, Apr. 2019.
[43] J. Li, A. M. Gee, M. Zhang, and W. Yuan, "Analysis of battery lifetime extension in a SMES-battery hybrid energy storage system using a novel battery lifetime model," *Energy*, vol. 86, pp. 175–185, Jun. 2015.
[44] J. Lofberg, "YALMIP: A toolbox for modeling and optimization in MATLAB," in *Proc. IEEE Int. Conf. Robot. Autom.*, Sep. 2004, pp. 284–289.

**YUNFEI BAI** (Student Member, IEEE) received the B.Eng. degree in vehicle engineering from the Beijing Institute of Technology, Beijing, China, in 2018, where he is currently pursuing the master's degree with the Department of Vehicle Engineering. His major research interests include electric vehicles, energy management systems, hybrid energy storage, and electrical power systems.

**JIANWEI LI** (Member, IEEE) received the B.Eng. degree from North China Electric Power University and the master's and Ph.D. degrees from the University of Bath, U.K. He was a Postdoctoral Researcher with the University of Liege, Belgium, a Researcher with the University of Oxford, U.K., and an Assistant Professor with the Beijing Institute of Technology. His research interests include electrical energy storages and hybrid energy storages, electrical vehicles, machine learning for energy storage systems, and microgrids.

**HONGWEN HE** (Senior Member, IEEE) received the M.SE. degree from the Jilin University of Technology, Changchun, China, in 2000, and the Ph.D. degree from the Beijing Institute of Technology, Beijing, China, in 2003, all in vehicle engineering. He is currently a Professor with the National Engineering Laboratory for Electric Vehicles, School of Mechanical Engineering, Beijing Institute of Technology. He has published more than 100 articles and holds 20 patents. His research interests include power battery modeling and simulation on electric vehicles, design, and control theory of the hybrid power trains.

**RICARDO CANELOI DOS SANTOS** (Member, IEEE) received the B.Sc. degree from Santa Cecilia University, Santos, Brazil, in 1996, and the M.Sc. and Ph.D. degrees from the University of Sao Paulo, Brazil, in 2000 and 2004, respectively, all in electrical engineering. In 2006, he joined the Federal University of ABC, Santo Andre, Brazil, where he is currently an Associate Professor with the Center for Engineering, Modeling and Applied Social Sciences. In 2014, he was a Postdoctoral Researcher with the University of Bath, Bath, U.K. His main research interests include power systems protection, artificial intelligence applications in power systems, distributed generation, and smart grids.

**QINGQING YANG** (Member, IEEE) received the B.Eng. degree from North China Electric Power University, China, and the M.Sc. and Ph.D. degrees from the University of Bath, U.K. She worked as a Lead Engineer on the electrical engineering when she was in the Beijing Electric Power Research Institute, State Grid Corporation of China. She is currently a Lecture with Coventry University. Her research interests include HVDC control and protection, virtual inertia in the power systems and artificial intelligence applications in energy storage, and smart grids.